Soltaniasl, Mohammad; Kawanishi, Kiyoshi; Maghrebi, Mahmoud F.; Razaz, Mahdi

Salt Intrusion and Water Circulation in a small Multi-Channel Estuary

SALT INTRUSION AND WATER CIRCULATION IN A SMALL MULTI-CHNNEL ESTUARY

Mohammad Soltaniasl [1], Kiyoshi Kawanishi [2], Mahmoud F. Maghrebi[3] and Mahdi Razaz [4]

ABSTRACT

In the upstream part of an estuary the gravitational circulation is an important mechanism. In this study, the intertidal measurement of salinity and current velocity over three tidal cycles have been analyzed. It is shown temporal and transversal pattern of bottom and surface salinity has an asymmetry and phase lag between the deepest and shallower regions. During the first portion of the ebb tides the tidal mixing contributes to decrease the stratification whole the cross-section. While, during the later portion of ebb tides the stratification was enhanced by the straining process. The results indicated the variations of shear velocity has more important role in the vertical and transversal variations of the Richardson number. The shear component is directed landward during all period of observation and has an important contribution comparing with the advection term. Also an asymmetry occurred in variations of shear terms at the shallowest and deepest regions

1. INTRODUCTION

An estuary is a transport link between a river and a sea. Therefore, it has characteristics of both the river and the sea. Tides transport saltwater in and out of an estuary and mix it with freshwater. There are several mixing mechanisms that vary in importance depending on the shape of the estuary, the location, the level of stratification, the density, and the strength of the tide. Tide-driven and density-driven (or gravitational circulation) are the most important mechanisms for the mixing process in an estuary (Savenije, 2005). In the upstream part of an estuary due to the large salinity gradient the gravitational circulation is an important mechanism while, in the tidally dominated estuaries the tide-driven mixing has a significant role throughout the estuary. These mixing mechanisms can be decomposed into many smaller constituting fluxes. The salt transport in an estuary is largely a balance between seaward advective flux, resulting from freshwater, tending to drive salt out of the estuary; and landward dispersive fluxes, tending to drive salt landward (upstream) due to triple-correlation between tide, velocity and salinity. The salt decomposition method can be contributed to

[1] PhD Student, Department of Civil and Environmental Engineering, University of Hiroshima, Kagamiyama 1-4-1, Higashi, Hiroshima, 739-8527, Japan (d101090@hiroshima-u,ac.jp)
[2] Associate Professor, Department of Civil and Environmental Engineering, University of Hiroshima, Kagamiyama 1-4-1, Higashi Hiroshima, 739-8527, Japan (kiyosi@hiroshima-u,ac.jp)
[3] Professor, Department of Civil and Environmental Engineering, University of Mashhad, 91775-1111, Iran, (maghrebi@ferdowsi.um.ac.ir)
[4] Assistant Professor, Department of Civil and Environmental Engineering, University of Hiroshima, Kagamiyama 1-4-1, Higashi Hiroshima, 739-8527, Japan (mrazaz@hiroshima-u,ac.jp)

the understanding of estuarine mixing processes, especially to investigate dominant mechanisms in a particular estuary in the presence of complicated coastline and topographical features.

The Ota Estuary is situated at Hiroshima City in Japan (Figure 1). Recently a new method for measuring the cross-sectional averaged velocity and salinity which is called Fluvial Acoustic Tomography System (FATS) has been developed (Kawanisi *et al,* 2010; Kawanisi *etal,* 2012). The FATS was deployed at the shallow tidal channel with large changes of water depth and salinity. This measuring method has some advantages compared to competing techniques, namely accurate measurement of cross-sectional mean velocities and salinity over a long duration. Our previous studies based on the FATS results, have indicated the tidal trapping, sloshing and tidal pumping are the significant dispersive fluxes. However, due to lack of deviation component from the cross-sectional averaged velocity and salinity the estimation of steady shear flux that results from the gravitational circulation, was not feasible. FATS measuring station is located near the bifurcation of the Ota Estuary (Figure 1). In this section due to the interaction between the freshwater and tide the vertical gradient of the salinity and velocity is varied temporarily during a tidal cycle. Also bathymetry changes and the effect of gate operation across the site study caused circulation and the transversal variations in the velocity and salinity.

Based on the measurement details of the water velocity and density the purposes of present study are to investigate the intertidal variations and cross-sectional distributions of the velocity, stratification and shear components during a tidal cycle.

2. STUDY AREA

The Ota River estuary encompasses the branched section of the Old Ota River and the Ota diversion channel about 9 km upstream (Figure 1a). The designed flood discharge in the Ota river floodway and the Old Ota River are 4500 and 3500 m3/s, respectively (Gotoh *et al,* 2010). The freshwater runoff into the diversion channel and Old Ota River is usually controlled by the array of floodgates, located near the bifurcation.

The Oshiba-Floodgate, located in the Old Ota River, consists of a fixed weir and a movable weir with three gates (Figure 1a). These gates always are completely opened. The Gion Floodgate which is located in the diversion channel consists of three movable sluice gates, of which usually only one sluice gate is opened slightly in order to make a stream cross-section of 32m×0.3m for spilling water. The inflow discharge is about 10-20% of the total flow rate of the Ota River on normal days (Kawanisi *et al,* 2010). The Yaguchi Gauging Station, which is located 14 km upstream from the mouth, is not tidally modulated. The Ota River discharge before the bifurcation can be estimated by using the rating curves in this station (Figure 1a).

During flood events, for discharge over 400 m^3/s at Yaguchi Station, all sluice gates of the Gion Floodgate are completely opened. A large scale flood occurred in September 2005, with a discharge about of 7200 m^3/s observed at this station (Gotoh *et al,* 2010). The water level fluctuations were measured at two stations in the estuary. The Kusatsu Station which is located at the mouth of the diversion channel. Also at the Gion Station which is located near the Gion Bridge (Figure 1a). The upstream border of the tidal compartment which shows the influenced distance of the tides, in the Ota River estuary is located about 13 km upstream far from the mouth (Figure 1a). The tides are primarily semidiurnal, but mixed with a diurnal component. The tidal range at the site study varied in a range from 0.3 m to 3 m during neap and spring tides, respectively.

3. INSTRUMENTS AND METHODS

3.1 The Schedule of the Observations

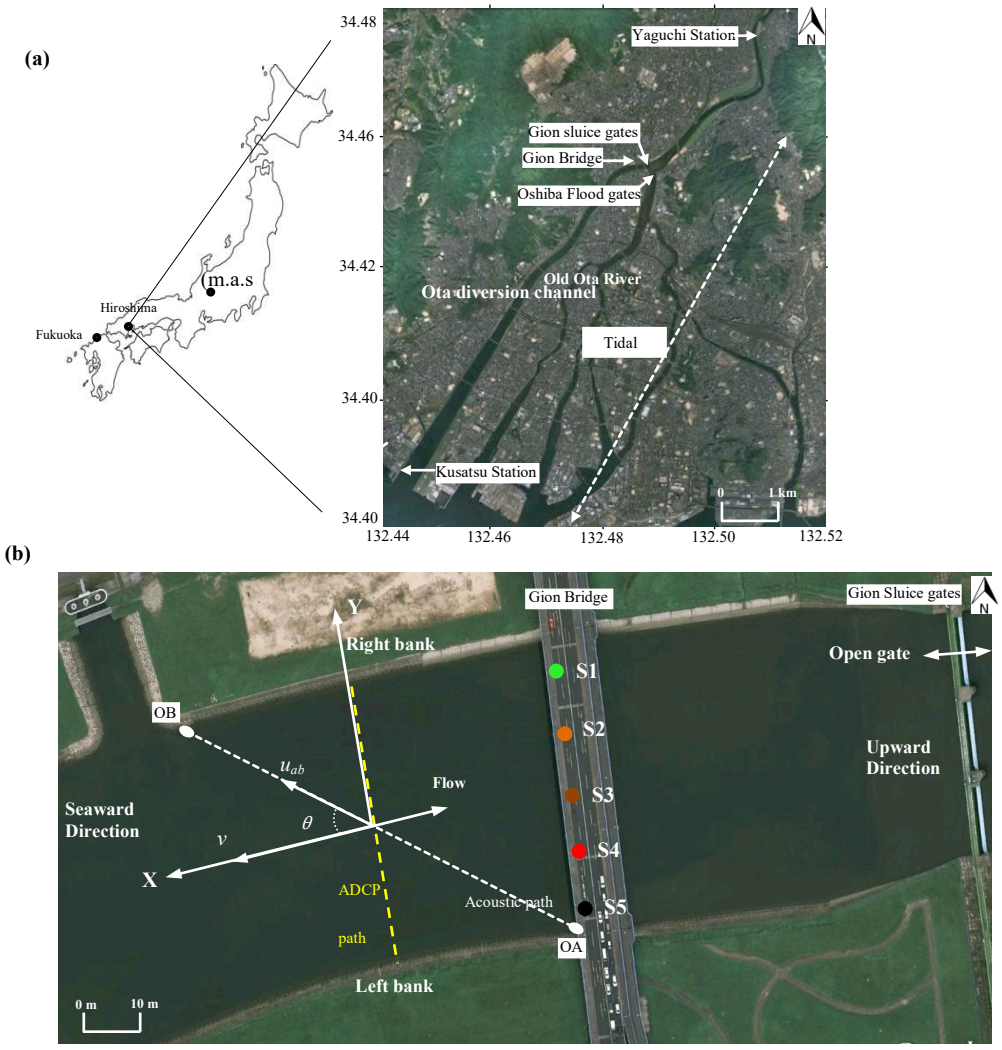

Figure 1 Study discharge (circles) estimated by WHADCP, (thick line) estimated by FATS area: (a) general view of site area and, (b) details of measurement section (Gion Station)

The field site was located 245m downstream of the Gion sluice gates (Figure 1b). Based on the bathymetry data of the Japan Ministry of Lands the mean depth, width, and bed slope of the site area are about 2.3m, 125m, and 0.04%, respectively. The cross-section of the channel in the site study has a trapezoidal shape with a deeper zone near the left side. As well, the tidal range at the site varied in a range from 0.3 m to 3 m during neap and spring tides, respectively (Gion Station).

We conducted an observation during spring tide condition on 25-26 January. The continuously and periodically measurements of the velocity were made using FATS and a moving boat, 1.2-MHz Teledyne RDI WorkHorse Acoustic Doppler Current Profiler (WHADCP), respectively. For removing the trajectory error, WHADCP was connected to a cable which mounted between the right and left shores of the field site. For this study all velocity vectors which estimated by the FATS and

WHADCP rotated into river coordinates (X, Y) in which the seaward direction is positive (Figure 1b).The vertical coordinates Z, is generally taken as following the mean sea level variations in the Ota Estuary.

The salinity profile was made using Alec Electronic Compact-CTD (conductivity-temperature-depth profiler) at the five stations from the Gion Bridge in the equal distance during the observation periods, so the lateral as well as temporal variability of the salinity distribution can be analyzed. The stations are shown by circles (Figure 1b).The vertical interval of salinity samples for these profiles is 0.1m, and the salinity measuring error is approximately 0.007. Notice here that presently we do not need to notify [psu] as a salinity unit, i.e. the practical salinity adopted by the UNESCO/ICES/SCOR/IAPSO Joint Panel on Oceanographic Tables and Standards does not have dimension. Moreover, the temporal mean salinity of the cross-section was estimated using the FATS which is explained in the next sections.

3.2 Estimating the Temporal velocity and salinity using FATS

FAT is an abbreviation for Fluvial Acoustic Tomography. The measurement principle of the FATS is the same as that used in an Acoustic Velocity Meter (AVM) which cross-sectional averaged velocity along the transmission line is calculated by using the ‘‘travel time method” (Sloat and Gain, 1995). In other words, the FAT system can estimate the mean cross-sectional velocity using the multi-ray paths which cover throughout the cross-section. The advantages of this method comparing with the current measuring systems were discussed by Kawanisi *et al,* (2012). Hereafter, the expression “FATS” denotes the name of this self-recorder instrument. The present studies of using FATS have indicated the noticeable reliability and accuracy of this innovative method for the long-term measurement of the velocity and salinity in both freshwater and tidal rivers (Kawanisi *et al,* 2010, and Kawanisi *et al,* 2012). As presented in (Figure 1b) a couple of FATS’ transducers with central frequency of 30 kHz were installed diagonally on both sides of the Ota diversion channel near the Gion Bridge to continuously measure the cross-sectional averaged velocity and salinity since 2008 until now.

Based on the measuring principles of FATS the cross-sectional average velocity in the direction of stream flow is estimated by the following formula:

$$v = \frac{u}{Cos\theta} \tag{1}$$

Where, u is the velocity along the ray paths and θ is the angle between the ray path and the stream direction which was 30° for these observations. The mean discharge at the site study cross-section (Y axis) is calculated as the product of the mean velocity and the channel cross-sectional area as:

$$Q = A(h)v\ Sin(\theta) \tag{2}$$

Where, h is the water depth. The cross-sectional averaged salinity can be estimated from the sound speed measured by FATS, temperature and water level variations (Medwin, 1975) as:

$$s = 35 + \frac{1449.2 + 4.6T - 0.055T^2 + 2.9\times10^{-4}T^3 + 0.016h - c}{(0.01T - 1.34)} \tag{3}$$

Where, *s* is salinity, *T* is temperature (°c), and *c* is the sound speed (*m/s*).

3.3 Tidal Shear Components

In general, the total salt flux in a cross-sectional width can be estimated as:

$$F_s = \int_0^h vsdz \tag{4}$$

Where, v and s is the temporal velocity and salinity components, h is the water depth and z is vertical coordinate. The temporal velocity and salinity profiles can be decomposed as $v = \bar{v} + v'$ and $s = \bar{s} + s'$, where the overbar and prime quantities represents depth-averaged and vertical deviation from the depth-averaged values, respectively. By substitution of decomposed components into Eq. (4) the new form of this equation can be written as:

$$F_s \approx \bar{v}\bar{s}\bar{h} + \overline{v's'}\bar{h} \tag{5}$$

Where, on the right-hand side of equation first term is the advective flux due to water discharge and the second term arising from the instantaneous deviation from the mean cross-sectional values.

4. RESULTS AND DISCUSSIONS

4.1 Temporal Variations in Salinity and Velocity

The vertical profile of the salinity in the site area was casted in five stations from the Gion Bridge (Figure 1a). In order to make the salinity profiles at cross-section of the ADCP path (Y axis) the data from each station in Gion Brige were objectively moved onto the Y-coordinate. Due to the near distance of the Gion Bridge from ADCP path (65 *m*), the vertical profile of the salinity was assumed to have the same trend as that measured at the Gion Bridge and was stretched or compressed to match the local depth.

WinRiver II software computes total volume discharge for each ADCP ensemble. The uncertainty in the discharge estimate arises from random errors, biases, and missed data (near the surface and bottom, and near the sides of a channel). The algorithm for estimating discharge is adopted from Simpson and Oltmann (1990), and Gordon (1989). Total Q, is the summation of discharge in the top, measured, bottom, left, and right layers. The highest contribution of bottom, near shore and top discharge in the total discharge were 7.5%, 2.2% and 1.1% during whole observation which did not significantly bias the ADCP results.

In order to compare the temporal salinity results of FATS and compact CTD we assumed the cross-sectional averaged salinity using the compact CTD data can be estimated by:

$$S_{CTD} = \frac{1}{A}\sum_i^n S_i A_i \tag{6}$$

where S_{CTD} and n are the mean salinity of the cross-section and the number of salinity samples that were collected by the compact CTD, respectively. Figure 2 depicts the temporal variations in

salinity, velocity and discharge according to FATS, Compact CTD and ADCP. Also the relations between the results and the error variations are presented in Figure 3, which the relative linear regression equations can be presented as:

$$S_{CTD} = 1.06 S_{FAT} - 0.24 \qquad R^2 = 0.91 \tag{7a}$$

$$v_{ADCP} = 0.695 v_{FAT} + .01 \qquad R^2 = 0.73 \tag{7b}$$

$$Q_{ADCP} = 0.685 Q_{FAT} + 2.9 \qquad R^2 = 0.78 \tag{7c}$$

The maximum differences between FATS and Compact CTD results occurred for salinity values less than 3. While, for the greater amounts of salinity the relative errors varied within ±10% (Figure 2a). The relative error of velocity results during the flood tides exceed 20% .However, the relative error of discharge results for noticeable range of variations estimate is ±15%. The results indicates that the differences between FATS and ADCP increase during the flood tides that can caused due to variations in the flow direction and water circulation at the study area which will be discussed later.

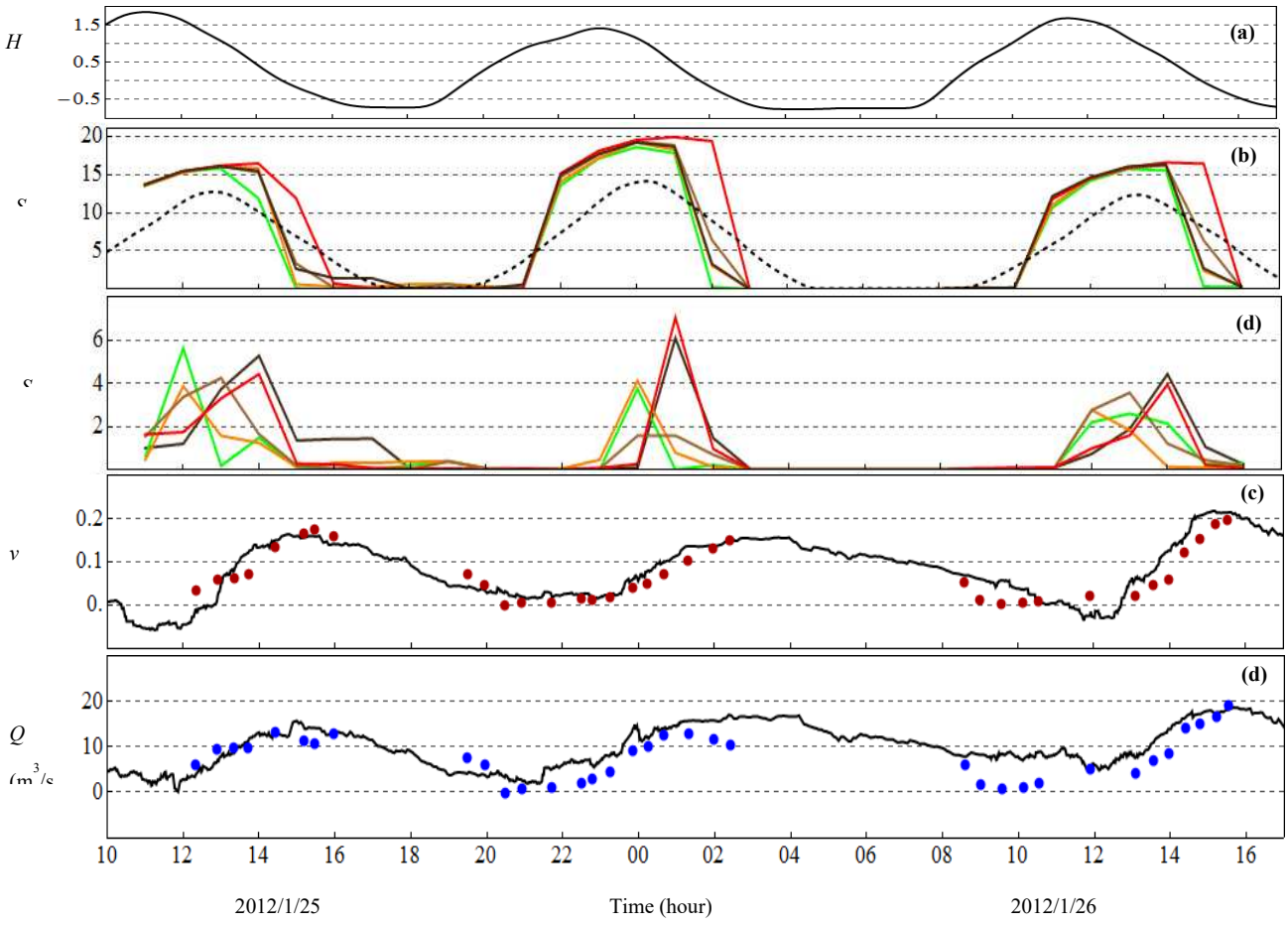

Figure 2 Time series of: (a) water level at Gion station, (b) bottom, (c) surface salinity at the stations casted by Compact CTD, S1 (green line), S2 (orange line), S3 (brown line), S4 (red line) and S5 (black line), the cross-sectional averaged salinity (black dashed line) estimated by FATS, (d) mean velocity (circles) estimated by WHADCP, (thick line) estimated by FATS (e) mean

4.2 Surface and bottom salinity structure

As mentioned before, the vertical interval of the salinity samples is 0.1 m. In this study, we purposed the salinity at the 0.1m below the water surface and above the bottom of the channel as the surface and bottom salinity, respectively.

Figure 2b indicates the temporal variations in surface, bottom and cross-sectional averaged salinity during the observation period. Stations 1 and 2 are front of the open sluice gate near the right shore and the station 4 located at the deepest region of the cross-section in the left shore, respectively (Figure 1b). In this channel, as in other tidal channels and estuaries, there is a phase lag between the water level, velocity and salinity. As shown, in all stations both bottom and surface salinity exceeded to the highest level after high water condition. The increasing pattern of bottom salinity at the stations was similar during the whole flood tides. However, during the ebb tides the saline water at the deepest region (S4) left from the cross-section around 30 min later than shallower sections. The pattern of surface salinity variations at stations indicates an asymmetry and phase lag. The surface salinity of S1 and S2 has a simultaneous trend and there is a similar condition for S4 and S5.

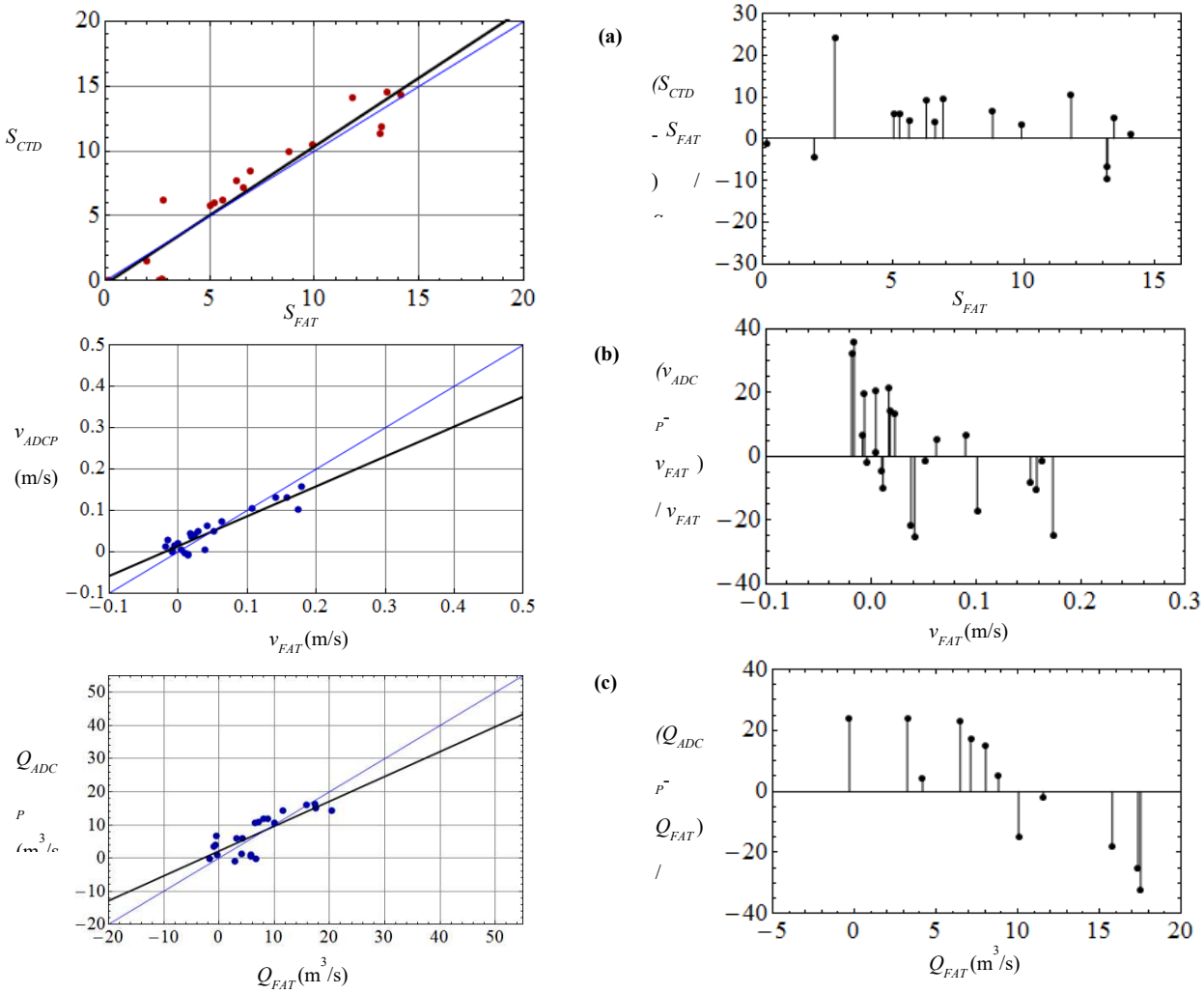

Figure 3 Relation between the cross-sectional averaged values and relative errors variations of: (a) salinity of FATS and compact CTD, (b) velocity of FATS and WHADCP, (c) discharge of FATS

The contour plot of the salinity and velocity at the cross-section of ADCP path, between hours 22 pm and 2 am (second tide) is plotted in Figure 4. On hour 22, the current at the upper depths (0.25 m.a.s.l < z) is directed seaward by the highest velocity at the right shore (0.05 m/s). In contrast, in the lower depths, saline water directed landward gradually by the velocity around -0.05m/s. On the high water level situation (hour 23) the cross-section indicating a uniform highly stratified condition. In this situation the velocity near the surface region of the right shore is progressively developing to the left shore (Figure 4b.2). On hour 1, salinity developed throughout the cross-section and similarly, the velocity counters contributed a two layer flow which the bottom-top velocity differences (Δv) peaks above a value of 0.29 m/s. Finally, during the end of ebb tide (hour 2) the core of velocity contours moved to the left shore and saltwater was limited at the deepest region of cross-section.

4.3 Evaluation of the stratification

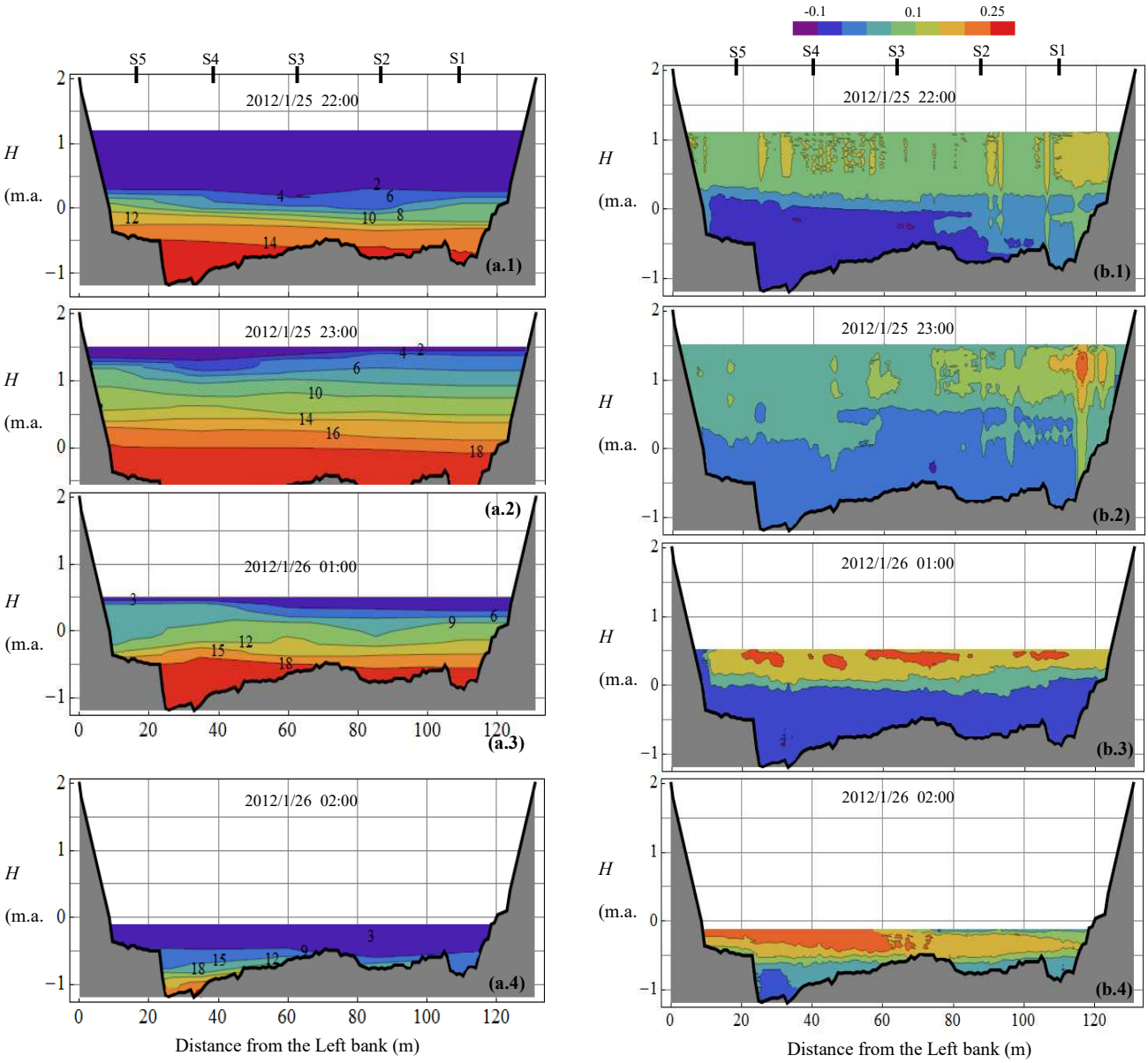

Figure 4 The cross-sectional counter plot of, (a) salinity, (b) velocity (m/s) during the second

Simpson *et al,* (1990) denoted that the degree of stratification in an estuary is established primarily by the interaction of two competing mechanisms: the stratifying effects of tidal straining tending to increases stratification during ebbs, decreases during floods, and the effects of tidal mixing which always decreases stratification. The gradient Richardson number which represents the relative importance of gravitational circulation compared to tidal mixing is defined as:

$$R_i = -\frac{g}{\rho}\frac{\partial \rho / \partial z}{(\partial v / \partial z)^2} \tag{8}$$

Where ρ is density (kg/m^3), g is the acceleration of gravity (m/s^2), v is velocity (m/s), and z denotes vertical coordinate. It indicates the tendency of the water column to either mix or resist mixing.

Here, to characterize the stratification variations during a tidal cycle we used a dimensionless representation of mixed layer thickness (MacDonald et al. 2008) as:

$$\psi = \frac{1}{2}\frac{h}{L_{50}}, \qquad L_{50} = h_{75} - h_{25} \tag{9}$$

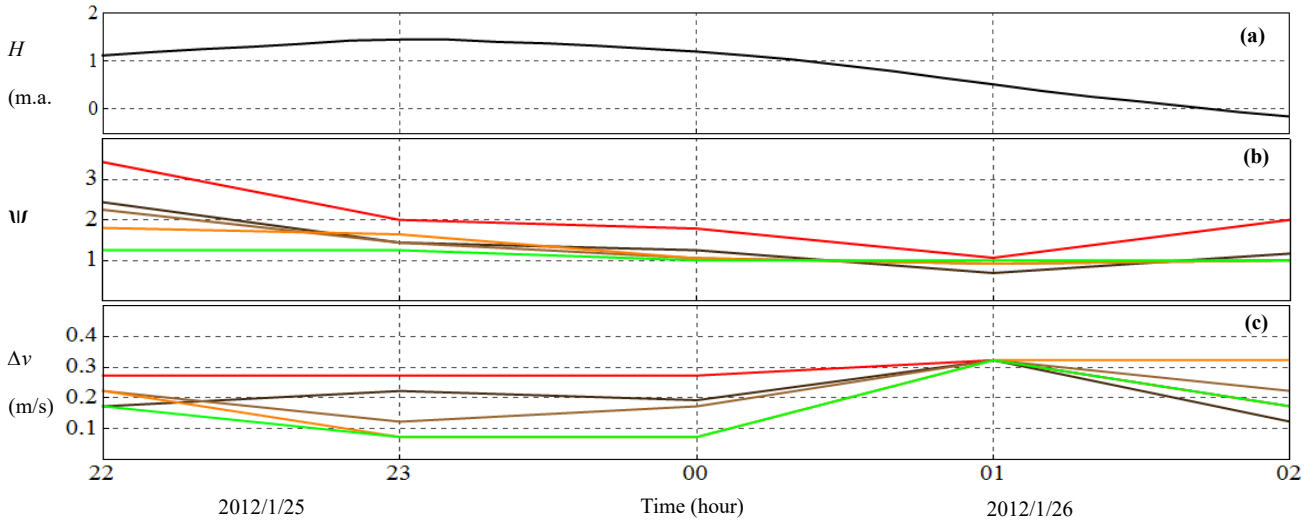

Figure 5 Variations of: (a) water level, (b) stratification parameter, (c) velocity differences between upper and lower layer at the stations during the second tide. In these figures, S1 (green line), S2 (orang line), S3 (brown line), S4 (red line) and S5 (black line)

Where h represents the local water column depth, and L_{50} represents the vertical distance between the 75th (h_{75}) and 25th (h_{25}) percentiles of the cross-section depth (i.e. where salinities typically range from 0 to 30, L_{50} at any location is the vertical distance between the 7 and 21 isohalines). The stratification parameter, ψ, can be interpreted as a continuum from well mixed conditions at $\psi < 1$ to highly stratified conditions at $\psi > 1$.The temporal change in the dimensionless stratification parameter can be related to the sum of straining and mixing terms (MacDonald *et al,* 2008). Moreover, in this paper, we defined the vertical velocity shear (Δv) as difference between the maximum landward-seaward velocities at the water column. The variation of ψ and Δv through the second tidal cycle (from hour 19 to hour 3) at stations is presented in Figure 5.

The high stratification parameter of the stations near the end of flood tides (hours 22 and 23) indicates highly stratified situation during end of floods. Throughout the ebb tide the stratification parameter ψ was gradually reducing and limit to a value of 1 approaching a more partially mixed situation at the hour 1. Noticeable differences in the temporal variations of the stations are also observed. At the deepest part of cross-section (S4) this parameter noticeably is greater than the shallower section during whole the tide. The evolution of Δv through the tidal cycle reveals a pronounced difference between the deeper and shallower sections of the cross-section. In the S1, Δv decreased to the value of 0.073 m/s during the middle of ebb tide. In contrast, the variation of this parameter at the deepest section (S4) approximately increased by the value of 0.29m/s. The variations of ψ and Δv at the stations suggest that during the later portions of the flooding (after hour 22) the tidal mixing contributes to decrease the stratification whole the cross-section and the stratification parameter was depressed to the minimum level at hour 1. Eventually, during the later portion of ebb tide (after hour 1) the stratification was enhanced by the straining process. Uncles *et*

al, (1990) proposed that within the tide, maximum stratification occurred around low water and minimum stratification around high water.

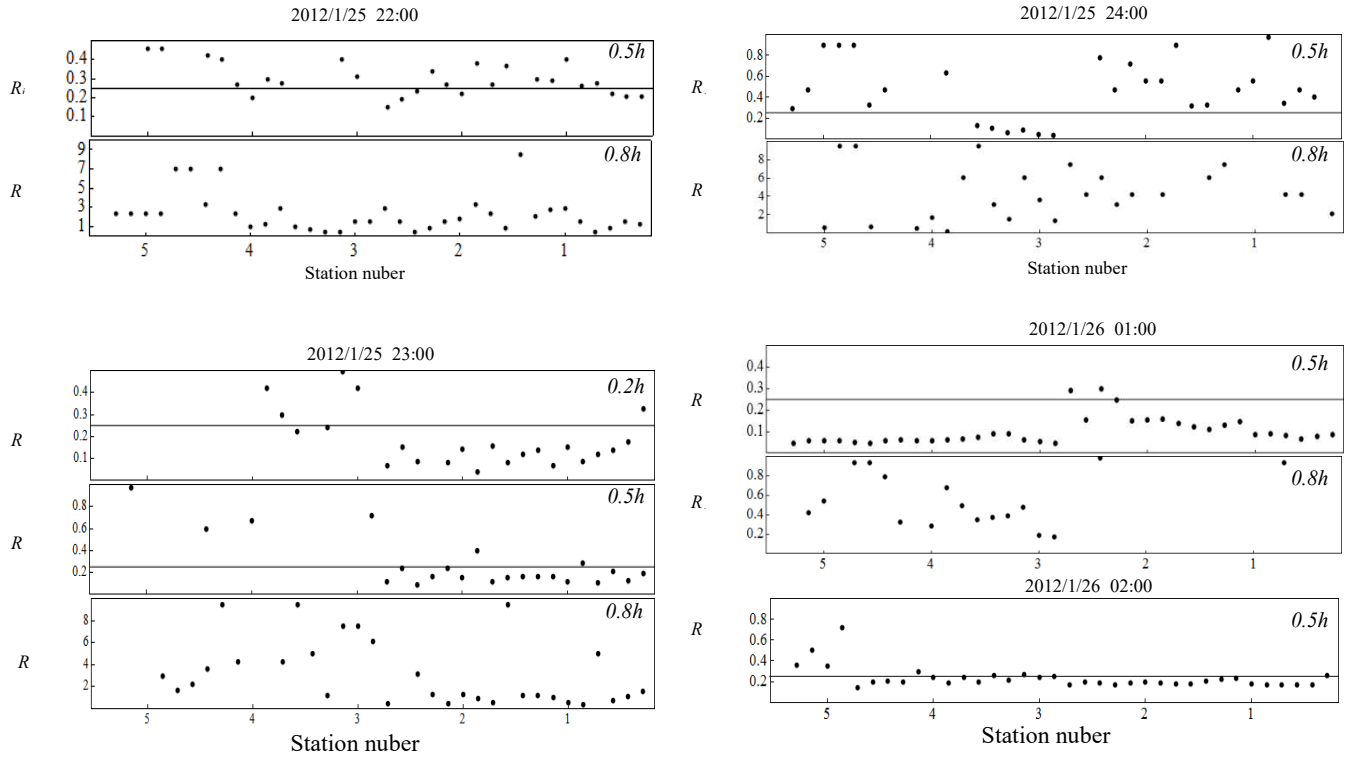

Figure 6 Transverse variations of Richardson number during second tide. In this figures, "*h*" is water depth and 0.2*h*, 0.5*h*, 0.8*h* denote the height below the water surface

The relative importance of the velocity shear in affecting stratification can be quantified in terms of the Richardson number. The variation of Richardson number through the second tidal cycle is presented in Figure 6. On hour 22, $dS/dz < 0.5$ in upper layer which is separated by a pycnocline, and around the mid-depth of channel ($z \approx 0$ m.a.s.l) due to high ratio of dv/dz the Richardson number is small and R_i tend to large values at the lower layer due to increasing in density and depressing in shear velocities. During the high water situation the low R_i region near the surface of right shore is caused by the greater shear velocities in this section. However, at the left side the R_i is large. Exempt from end portion of ebb tide, the temporal variations in salinity gradient at whole cross-section is approximately same and so the structure of shear velocity has important role in variations of the Richardson number. The magnitudes of R_i near the boundary layer of upper seaward and lower landward flow (the depth ≈ 0.5h) is varied around 0.25.While,in the near-bottom layer due to high stratification and less values of Δv, R_i significantly increased.

4.4 Estimation of Shear Components

There are two methods for analyzing a series of salt fluxes measurements. In the first method it is assumed that the primary variations are in the transverse direction, and the transverse deviations are evaluated before the vertical ones. In the second method the vertical deviations are the primary variations (Dyer *et al,* 1992; Uncles *et al,* 1990; Hughs and Rattray 1980; Fischer, 1972). Based on this aspect, the partitioning of the shear effect can be considered into transverse and vertical

components. Moreover the transverse contributions to the shear dispersion of salt were small in a highly stratified estuary, whereas in partly mixed estuaries the transverse and vertical shear contributions were comparable. Lerczak and Geyer (2006) pointed out that the various mechanisms may be responsible for the downgradient flux of salt in estuaries. They distinguish between steady shear dispersion resulting from the combination of straining the salinity field by vertically or laterally sheared subtidal currents and vertical or lateral mixing, and tidal oscillatory salt flux, resulting from tidal correlations between longitudinal currents and salinity variability. In this study we estimated the shear components for each station using Eq. (5).

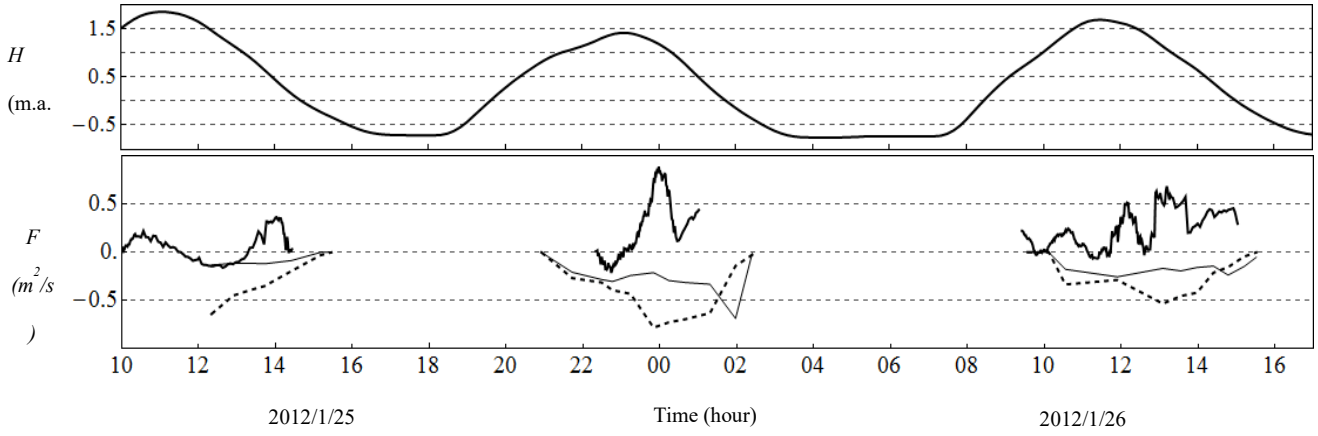

Figure 7 Variations of (a) temporal water level at the Gion Station; (b) advective term (thick line), shear flux at station 1 (dashed line) and shear flux at station 4 (thin line)

As mentioned the reflection of transmitted ADCP signals from the channel bottom causes interference by acoustic side lobes and increases the uncertainty of near-bed velocities. Therefore, in this study, the velocities were extrapolated by fitting the near-bottom ADCP data to a log-layer profile.

In Figure 7, the variations of advection and shear components are presented. In this figure, the seaward direction is positive. The advection and shear terms were estimated using FATS, ADCP and Compact CTD data, respectively. The cross-correlation between the velocity, salinity and water level is important in variations of this component. As it can be seen, the advective flux is mostly seaward and exceed to the highest level during first portion of the ebb tides. Moreover, as it discussed before, the stratification was reduced during the ebb tides (Figure 5a). This suggests that the main factors decreasing the stratification during the ebb tides are the advection process and vertical mixing. However, the straining is significant mechanisms to increase the stratification during flood tides. In order to consider the importance of transversal variations in shear components, this flux was estimated at the station1 and 4. The results indicated noticeable differences between the variation of shear components of station 1 and 4. Overall, the shear component is directed landward during all period of observation and has an important contribution comparing with the advection terms. During the second tide (hour 21-02), the shear component at Station 1 exceed to the highest level by the value of $-0.73 m^2/s$ at the first portion of ebb tides. While, the station 4 experienced the maximum value of $-0.62 m^2/s$ at the end portion of ebb tide. This asymmetry in variations of shear components is resulted from temporal and spatial variations in the stratification and shear velocities.

5. CONCLUSIONS

In this study, the intertidal variations in the salinity and velocity in the upstream part of a shallow estuary was investigated. The measurements of the velocity were made using FATS and a moving boat WorkHorse Acoustic Doppler Current Profiler (WHADCP) and the salinity profile was from five stations along the site study cross-section during the observation periods. The results indicate that the differences between FATS and ADCP increase during the flood tides which is caused due to variations in the flow direction and water circulation at the study area.

The increasing pattern of bottom salinity during the flood tides at the whole cross-section was similar. However, during the ebb tides the saline water at the deepest region (S4) left from the cross-section around 30 min later than shallower sections. The pattern of surface salinity variations at stations indicates an asymmetry and phase lag between the deepest and shallower regions.

The variations of stratification parameter ψ and the shear velocity Δv at the stations suggest that during the later portions of the flooding the tidal mixing contributes to decrease the stratification whole cross-section. While, during the later portion of ebb tides the stratification was enhanced by the straining process.

The Richardson number through the second tidal cycle indicated noticeable temporal and spatial variations. Except from end portion of ebb tide, the temporal variations in salinity gradient at whole cross-section is approximately same and so the structure of shear velocity has important role in the vertical and transversal variations of the Richardson number. The magnitudes of R_i near the boundary layer of upper seaward and lower landward flow is varied around 0.25.While,in the near-bottom layer due to high stratification and less values of Δv, R_i significantly increased.

The shear component is directed landward during all period of observation and has an important contribution comparing with the advection term. The results indicated the highest values of shear terms at the shallowest and deepest regions occurred at the last and first portion of ebb tides, respectively. This asymmetry in variations of shear components is resulted from temporal and spatial variations in the stratification and shear velocities.

REFERENCES

Dyer, K.R. (1992) “The cross sectional salt balance in a tropical estuary during a lunar tide and a discharge event” Journal of Estuarine, Coastal and Shelf Science, Vol. 30, pp.579-591

Fischer, H. B. (1972) “Mass transport mechanisms in partially stratified estuaries”, Journal of Fluid Mech, Vol. 53, pp.671-687

Gordon, R. L. (1989), “Acoustic Measurement of River Discharge”, Journal of Hydraulic Engineering, Vol. 115, No. 7, pp.925-936.

Gotoh, T., Fukuoka, S., Abe, T. (2010) “Evaluating flood discharge and bed variation in the Ota River Floodway”, Proceedings of 9th International, ICHE conference, http://c-faculty.chuo-u.ac.jp/~sfuku/sfuku/03_paper/paper/ICHE2010-goto.pdf

Hansen, D. V., Rattray, M. Jr. (1965) “Gravitational circulation in straits and estuaries”, Journal of Marine Research, Vol. 23, pp.104-122.

Kawanisi, K., Razaz, M., Kaneko, A. and Watanabe, S. (2010), “Long-term measurement of stream flow and salinity in a tidal river by the use of the fluvial acoustic tomography system”, Journal of Hydrology, Vol.380, pp.74-81

Kawanisi, K., Razaz, M., Ishikawa, K., Yano, J and Soltaniasl, M, (2012), "Continuous measurements of flow rate in a shallow gravel-bed river by a new acoustic system", Water Resour. Res, [Accepted 16 April 2012, doi:10.1029/2012WR012064]

Lerczak, J.A., Geyer, W.R. (2006), "Mechanisms driving the time-dependent salt flux in a partially stratified estuary", Journal of Physical Oceanography, Vol.36, pp.2296-2311

Medwin, H. (1975), "Speed of sound in water: a simple equation for realistic parameters", Journal Acoustical Society of America, Vol.58, pp.1318.

MacDonald, D.J., Horner-Devin, A.R. (2008), "Temporal and spatial variability of vertical salt flux in a highly stratified estuary", Journal of Geophisical Research, Vol.113, C09022, doi:10.1029/2007JC004620

Savenije, H.H.G.(2005), "Salinity and tides in alluvial estuaries", Elsevier, Amsterdam, pp.109

Simpson, J.H., Brown, J., Matthews, J., and Allen, G. (1990), "Tidal straining, density currents, and stirring in the control of estuarine stratification", Estuaries, Vol.13, pp.125-132.

Simpson, M. R. and Oltmann, R. N. (1990). An Acoustic Doppler Discharge Measurement System. Proceedings of the 1990 National Conference on Hydraulic Engineering, Vol. 2, 903-908.

Sloat, J.V., Gain, W.S. (1995), "Application of acoustic velocity meters for gaging discharge of three low-velocity tidal streams in the St. John River Basin, Northeast Florida, US Geological Survey", Water-Resources Investigations Report, 95-4230. pp26

Uncles, R. J., Elliott, R. C. A. and Weston, S. A. (1985), "Observed fluxes of water, salt and suspended sediment in a partly-mixed estuary", Estuarine, Coastal and Shelf Science, Vol.20, pp.147–168